Wild, K., Bohner, T., Folkers, G.& Schulz, G.E. The structures of thymidine kinase from Herpes simplex virus type 1 in complex with substrates and a substrate analog. Protein Sci....

ARTICLE *in* PROTEIN SCIENCE · OCTOBER 2008

Impact Factor: 2.85 · DOI: 10.1002/pro.5560061005 · Source: PubMed

Protein Science (1997), 6:2097–2106. Cambridge University Press. Printed in the USA.

The structures of thymidine kinase from *Herpes simplex* virus type 1 in complex with substrates and a substrate analogue

KLEMENS WILD,[1,3] THOMAS BOHNER,[2,3] GERD FOLKERS,[2] AND GEORG E. SCHULZ[1]

[1]Institut für Organische Chemie und Biochemie, Albert-Ludwigs-Universität, Albertstrasse 21, 79104 Freiburg im Breisgau, Germany

[2]Department Pharmazie, Eidgenössische Technische Hochschule, Winterthurerstrasse 190, 8057-Zürich, Switzerland

(RECEIVED March 18, 1997; ACCEPTED May 28, 1997)

Abstract

Thymidine kinase from *Herpes simplex* virus type 1 (TK) was crystallized in an N-terminally truncated but fully active form. The structures of TK complexed with ADP at the ATP-site and deoxythymidine-5′-monophosphate (dTMP), deoxythymidine (dT), or idoxuridine-5′-phosphate (5-iodo-dUMP) at the substrate-site were refined to 2.75 Å, 2.8 Å, and 3.0 Å resolution, respectively. TK catalyzes the phosphorylation of dT resulting in an ester, and the phosphorylation of dTMP giving rise to an anhydride. The presented TK structures indicate that there are only small differences between these two modes of action. Glu83 serves as a general base in the ester reaction. Arg163 parks at an internal aspartate during ester formation and binds the α-phosphate of dTMP during anhydride formation. The bound deoxythymidine leaves a 35 $Å^3$ cavity at position 5 of the base and two sequestered water molecules at position 2. Cavity and water molecules reduce the substrate specificity to such an extent that TK can phosphorylate various substrate analogues useful in pharmaceutical applications. TK is structurally homologous to the well-known nucleoside monophosphate kinases but contains large additional peptide segments.

Keywords: dimer interface, nucleoside monophosphate kinases, sequence motifs, substrate specificity, X-ray analysis

It has been estimated that 60–95% of the world population is infected by members of the human *Herpes* virus family (WHO Meeting, 1985), especially by *Herpes simplex* virus type 1 (HSV-1) and type 2. The virus rests most of the time in a latent form in cells of the nervous system. On reactivation it can cause a variety of diseases like the common fever blisters, genital skin lesions, blindness, and encephalitis (Whitley & Gnann, 1993). The incidence of *Herpes* virus diseases in immuno-compromised people such as AIDS patients is particularly high. Here, the reactivation of a latent *Herpes* virus infection appears to be facilitated.

Numerous anti-*Herpes* drugs have been developed; they have been reviewed by De Clercq (1993). The initial target of these drugs is nearly in all cases the viral thymidine kinase (TK). This enzyme is part of the thymine salvage pathway, catalyzing the transfer of the γ-phosphate from ATP to the 5′-hydroxyl of deoxythymidine (dT) to form deoxythymidine-5′-monophosphate (dTMP). In contrast to the corresponding host cell enzyme, TK from HSV-1 is not very specific and phosphorylates its primary product, dTMP, as well as a variety of substrate analogues such as the uridine derivatives idoxuridine and brivudin or guanosine derivatives aciclovir and ganciclovir. The tolerance difference between viral and cellular thymidine kinases and the preferences of the viral DNA polymerase (Ilsley et al., 1995) are the basis for the efficacy of present drugs, as well as the basis for future developments, e.g., a virally directed prodrug therapy of malignant brain tumors (Culver et al., 1992). The therapeutic value of idoxuridine is limited, though, because it is also accepted by the cellular enzyme (Spadari et al., 1995). A preliminary structure of TK from HSV-1 was published earlier (Wild et al., 1995), followed by an independent second structure analysis of Brown et al. (1995). Now, we report the refined structures of three different forms of the ligated enzyme.

Reprint requests to: Georg E. Schulz, Institut für Organische Chemie und Biochemie, Albertstrasse 21, D-79104 Freiburg im Breisgau, Germany; e-mail: schulz@bio5.chemie.uni-freiburg.de.

Abbreviations: Aciclovir, 9-(2-hydroxyethoxymethyl)guanine; AK_{yst}, adenylate kinase from yeast; brivudin, (E)-5-(2-bromovinyl)-2′-deoxyuridine; dT, deoxythymidine; dTMP, deoxythymidine-5′-monophosphate; ganciclovir, 9-(1,3-dihydroxy-2-propoxymethyl)guanine; HSV-1, *Herpes simplex* virus type 1; idoxuridine, 5-iodo-2′-deoxyuridine(D-ribose); 5-iodo-dUMP, idoxuridine-5′-phosphate; NMP, nucleoside monophosphate; RMSD, root mean squares deviation; TK, thymidine kinase from *Herpes simplex* virus type 1, ATP, thymidine 5′-phosphotransferase (EC 2.7.1.21).

[3]Contributed equally to the results.

Table 1. *Data collection statistics of TK complexes*[a]

Complex with ADP and:	dTMP[b]	dT	5-iodo-dUMP
Resolution (Å)	10–2.75	100–2.8	100–3.0
Reflections, total	28,046	26,826	21,343
Redundancy	2.3	2.3	2.4
R_{sym}[c]			
Overall (%)	9.2	4.5	8.4
Last shell (%)	41.2	18.9	24.4
Completeness			
Overall (%)	89.5	83.1	77.1
Last shell (%)	91.2	63.7	49.8
Fraction $I > 3\sigma$			
Overall(%)	73.1	65.3	67.9
Last shell (%)	40.1	38.9	28.6

[a]The crystals of the complex with dTMP belong to space group $I4_1$ with cell axes $a = b = 83.4$ Å and $c = 156.7$ Å. The other crystals are isomorphous with axes differences below 1%.

[b]Collected using the synchrotron beamline X31 at the EMBL outstation (Hamburg).

[c]$R_{sym} = \Sigma_{h,i}|I(h)_i - \langle I(h)\rangle|/\Sigma_{h,i}I(h)_i$; the overall values concern the complete data sets as collected. The last shells comprise the resolution ranges 2.80–2.75 Å, 2.89–2.80 Å, and 3.16–3.00 Å for the complexes with dTMP, dT, and 5-iodo-dUMP, respectively.

Results and discussion

Refined structures

All three obtained crystal types are isomorphous and belong to space group $I4_1$ with one subunit of the dimeric enzyme in the asymmetric unit. The structure of TK had initially been solved by multiple isomorphous replacement at 3.0 Å resolution (Wild et al., 1995). For the refinement we now switched to a 2.75 Å resolution data set of higher quality (Table 1).

During the refinement we realized that the ligands were ADP and dTMP, although TK had been co-crystallized with ATP and dT under 1 mM EDTA. The finding was confirmed by paper chromatography (no ATP in the crystal), $(F_o - F_c)$-maps, and simulated annealing omit-maps. As a consequence, we revisited the earlier 3.0 Å resolution data set, which was based on a crystal grown under the same conditions but had not been rigorously refined. A thorough refinement of the old data now showed that this crystal also contained ADP and dTMP, not ATP and dT as previously reported. Obviously, the applied inhibitor EDTA had failed to remove the divalent cations required for catalysis completely. Some residual activity running over the four weeks between crystallization set-up and data collection (same time for old and new crystal) had phosphorylated dT in both of them.

TK is a homodimer with 376 residues per subunit. The crystallized recombinant TK comprised residues 34–376 and the model of complex TK:ADP:dTMP consists of 313 structured residues: ADP, dTMP, and 52 water molecules. Residues 34–45, 150–152, and 265–279 are missing due to insufficient electron density. Because these residues also are missing in the TK model of Brown et al. (1995), which was derived from a complete polypeptide chain crystallized in a different packing, we conclude that the observed segmental mobility is an intrinsic TK property. The lack of structure for residues 1–45 agrees with the observation that this segment is not required for catalysis (Halpern & Smiley, 1984). The enzyme structure is depicted in Figure 1. The secondary structures are defined in Figure 2.

Given these mobilities, we made sure that there were no artifacts introduced by declaring the molecular two-fold axis of TK as crystallographic, which reduces the density of all asymmetric parts. For this purpose, we assumed an asymmetric TK dimer in space group $P4_1$ with the same cell axes as $I4_1$, and analyzed the raw diffraction data in $P4_1$. Since this re-evaluation showed no significant intensities at the additional reflection positions, there is no regular asymmetry.

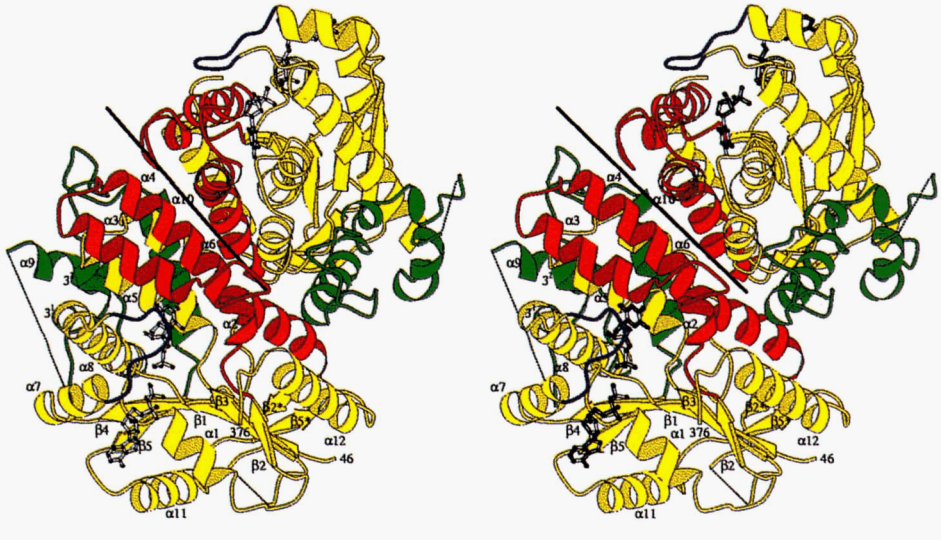

Fig. 1. Stereoview of the symmetric TK dimer with bound ADP and dTMP. The domains are defined according to the NMP-kinases as CORE (residues 46–81, 143–218, 227–250, 323–376, yellow), NMP_{bind} (82–142, red), and LID (219–226, blue). The 72 additional residues around position 290 are green. Mobile parts are given as dashed lines, the twofold axis is inserted, secondary structures are defined in Fig. 2.

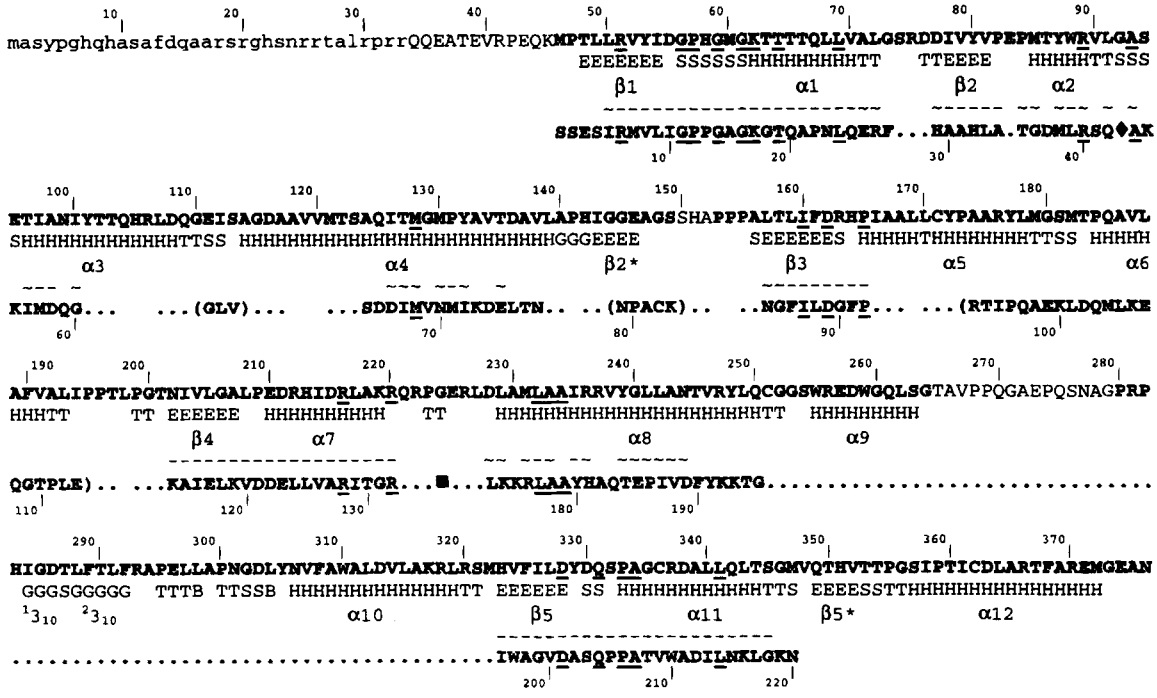

Fig. 2. Secondary structure assignment for complex TK:ADP:dTMP and the alignment with AK_{yst}. First line, numbered sequence of TK (McKnight, 1980), the truncated N-terminal residues are given in lower case letters, the residues included in the model are in bold type, residues identical to AK_{yst} are underlined. Second line, secondary structures of TK using program DSSP (Kabsch & Sander, 1983; H, α-helix; G, 3_{10}-helix; E, β-strand; S, turn without hydrogen bond; T, turn with hydrogen bond; B, bridge), the β-sheet nomenclature is adjusted to the NMP-kinases. Third line, structurally equivalent residues of TK and AK_{yst} with distances below 3 Å (−) and below 5 Å (~). Fourth line, numbered sequence of AK_{yst} with non-aligned parts in parentheses and two inserted segments removed for clarity: (♦) segment IAKGTQLGLE; (■) segment LIHPASGRSYHKIFNPPKEDMKDDVTGEALVQRSDDNADA.

In another analysis we collected a data set from TK co-crystallized with ATP, dT and EDTA under the same conditions as before but with an incubation time of 15 instead of 4 weeks. This analysis showed ligands ADP and dT; i.e., the γ-phosphoryl group of ATP was removed altogether. The time difference and the availability of Glu83 as an acid attacking the 5′-hydroxyl suggests that ATP had phosphorylated dT to dTMP (during the first 4 weeks), which then lost its phosphoryl group by hydrolysis over the remaining 11 weeks. The experiment was repeated using a second crystal with the same history, which additionally was soaked for 5 min (longer soaks destroyed the crystal) with 10 mM $MnCl_2$ before the data were collected. The result was the same, and thus we proceeded only with the more accurate Mn^{2+} soak (Table 1). The structure was solved by difference-Fourier techniques and refined, yielding complex TK:ADP:dT without Mn^{2+} (Table 2).

In a third analysis, we modified the protein isolation procedure, substituting dT with idoxuridine (K_i = 14 μM) and co-crystallized TK with ATP, additional idoxuridine, and 1 mM EDTA. A data set of a 4-week-old crystal was collected to 3.0 Å resolution (Table 1), giving rise to the structure of the complex TK:ADP:5-iodo-dUMP, which was subsequently refined (Table 2). Here again, the γ-phosphoryl group had been transferred to form the ester in spite of the presence of EDTA.

Quality of the models

In agreement with the obtained resolution, the coordinate errors remain in the 0.3–0.4 Å range (Table 2). *B*-factor refinements were

Table 2. *Refinement statistics of TK complexes*

Complex with ADP and:	dTMP	dT	5-iodo-dUMP
Resolution (Å)	10–2.75	10–2.8	10–3.0
Unique reflections	12,164	11,171	8,411
R-factor (%)	18.2	17.5	22.2
R_{free}[a] (%)	23.6	23.8	30.5
Number of atoms in			
Protein	2391	2391	2391
Substrates	48	44	48
Water	52	28	6
RMSD bond lengths (Å)	0.007	0.009	0.013
RMSD bond angles (°)	1.4	1.5	1.8
Error estimates (Å)			
Luzzati plot	0.27	0.27	0.32
Read-σ_A-plot	0.46	0.46	0.56
Mean *B*-factor (Å^2)			
Main chain	34	31	—[b]
Side chains	36	34	—
ADP	59	48	—
NMP/nucleoside	23	23	—
Water	35	30	—
RMSD *B*-factors (Å^2)			
Along bonds	7.1	6.6	—[b]
Along angles	9.1	9.3	—
Ramachandran quality[c] (%)	92	92	86

[a]The random test set comprised 10% of the data.
[b]*B*-factors were not refined and thus the same as for TK:ADP:dTMP.
[c]Residues in the "most favored region" (Laskowski et al., 1993).

performed cautiously with two structures but not applied to the complex TK:ADP:5-iodo-dUMP. They were justified as they caused the R_{free}-value to drop as much as the R-value. Because of extreme mobility, all three models lack N-terminal residues 34–45 as well as residues 265–279. Moreover, all of them have rather mobile segments around positions 73, 151, 221, 299, and at the C-terminus (see below). The structures of the bound ligands are well-defined in their densities (Fig. 3).

The (ϕ,ψ)-scatter plots of backbone dihedral angles show Ramachandran qualities of 86% or more (Table 2) that are above standard (Laskowski et al., 1993). Arg163 of the active center is always in the disallowed region around (80°, 150°). Its strained conformation appears to be important for catalysis (see below).

Dimer interface and crystal packing

The dimeric viral TK was suggested to be a homologue of the dimeric cellular deoxycytidine kinase (Harrison et al., 1991). In contrast, the human cytosolic thymidine kinase appears to be active as a homotetramer (Munch-Petersen et al., 1993). The dimer interface of TK has a buried solvent accessible surface area of 1800 Å^2 per subunit, which amounts to 14% of the total subunit surface. The interface approximates a circular plane with only one substantial protrusion formed by Trp310 anchoring in a hollow of the other subunit. The interface is dominated by helices: α4, α6, and α10 participate fully whereas α2 and α12 are partially involved (Table 3). With 65% hydrophobic, 26% polar, and 9% ionogenic residues, the interface is exceptionally non-polar (Jones & Thornton, 1995). All eight hydrogen bonds are located at the periphery. There is no salt bridge.

Table 3. *Dimer interface and crystal packing in complex TK:ADP:dTMP*

Contact[a]	Contact area (Å^2)	Contact partners[b]	Number of hydrogen bonds
I–II	1800	*a–a*	8
I–III	350	*b–c*	8
I–IV	350	*c–b*	8

[a]Using subunit I (x,y,z) as reference, the related subunits are II $(-x+1,-y,z)$, III $(y+\frac{1}{2},-x,z+\frac{3}{4})$ and IV $(y,-x+\frac{1}{2},z+\frac{1}{4})$.

[b]Contacting residues are those where the accessible surface area decreases by more than 1 Å^2 on association. The residue lists are: a = 87,91–93/119–120,122–123,126–127,130,133–135,137–138,140–141/183,185–186,188–190,192–193,195–196/305–308,310–311,313–314,317–318/364,367–368,371–372 (where slashes separate helix segments from each other); b = 102,105–106,108–109,111,226–229; c = 248,250–254,257–258,261,281–283.

In contrast to the large interface, the crystal contacts bury only 7% of the total dimer surface. These contacts direct the dimers to the observed very roomy arrangement with a solvent content as high as 67%, giving rise to mechanically labile crystals.

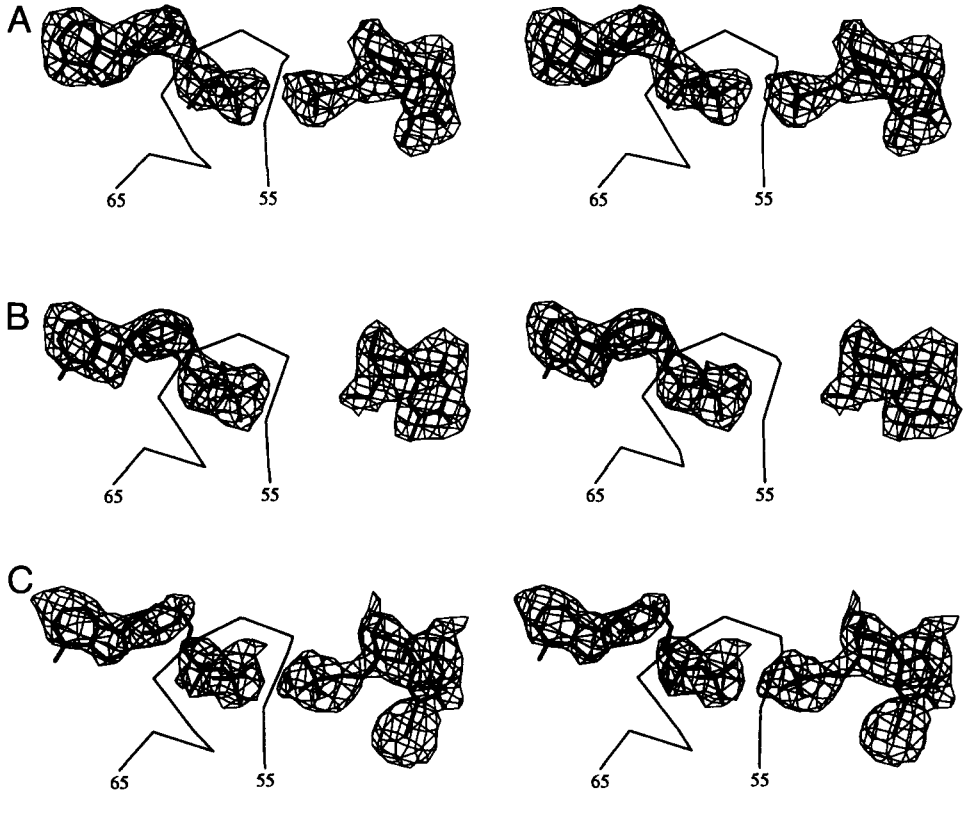

Fig. 3. Final $(2F_o - F_c)$-electron density maps for all substrates with the C$^\alpha$ trace of the P-loop as reference. All maps are contoured at the 1.0 σ level. **A:** ADP and dTMP at 2.75 Å resolution. **B:** ADP and dT at 2.8 Å resolution. **C:** ADP and 5-iodo-dUMP at 3.0 Å resolution.

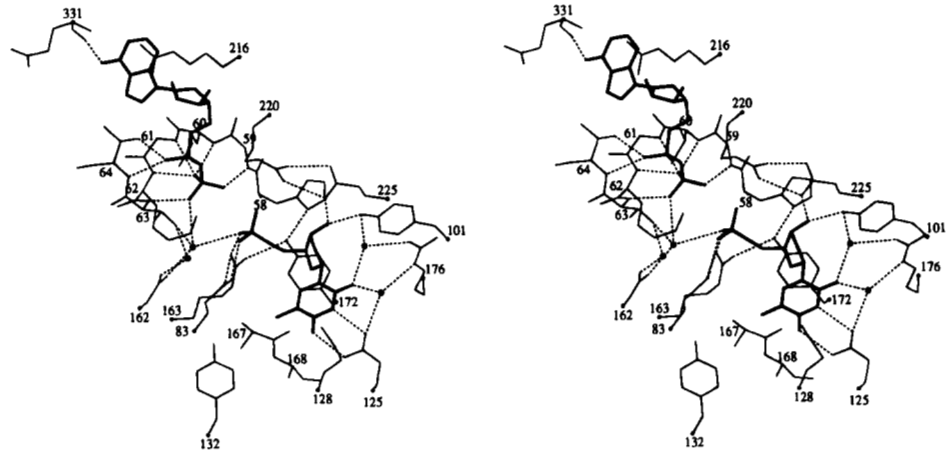

Fig. 4. Stereoview of the active center of TK with the substrates ADP and dTMP (thick lines). Hydrogen bonds are dotted. Several C^{α} positions are marked by dots.

The ATP/ADP-binding site

TK contains the sequence fingerprint (residues 56–63) for the giant anion hole (Dreusicke & Schulz, 1986) that accommodates the β-phosphate of ATP in numerous ATP-binding proteins (Schulz, 1992). The corresponding peptide fold is known as P-loop (Fig. 3). In all reported TK complexes, ADP binds in the expected mode at the giant anion hole (Fig. 4). The significant fingerprint residue Lys62, which was suggested to accompany the γ-phosphoryl transfer during catalysis (Müller & Schulz, 1992), has only weak density, possibly because of the missing γ-phosphate. Thr64 is the residue after the common fingerprint. It is important here as it forms two hydrogen bonds to the ADP α-phosphate. The adenine moiety of ADP makes only one hydrogen bond with the polypeptide, while the ribose moiety shows none at all (Fig. 5). As usual, adenine is sandwiched with a guanidinium group (Arg216 of α7).

Taken together, the adenosine moiety of ATP/ADP is only weakly bound as reflected in a rather high K_M value of 70 μM (Chen et al., 1979a) and in a low specificity; GTP, CTP, and their deoxy forms are accepted besides ATP (Kit, 1985). The enzyme probably can also use other di- and triphosphates like the nucleoside monophosphate (NMP) kinases, which process, for instance, thiamine diphosphate (Miyoshi et al., 1990).

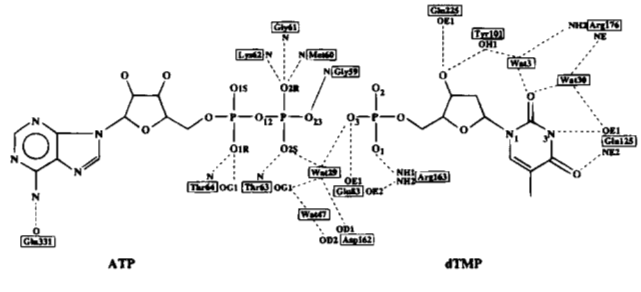

Fig. 5. Sketch of all hydrogen bonds to the substrates in complex TK:ADP:dTMP. Hydrogen bonds are defined by distances below 3.5 Å and angles above 120°. Complex TK:ADP:dT shows the following deviations from the presented scheme: Glu83 forms only one hydrogen bond, which is to 5′-OH of the ribose of dT; Arg163 is detached from dT and Glu83; and there are no equivalents for Wat29 and Wat47. In complex TK:ADP:5-iodo-dUMP only Wat30 is modeled.

The nucleoside/NMP-binding site

TK phosphorylates thymidine and thymidylate (Chen et al., 1979b; Maga et al., 1994). Apart from the ATP/ADP-site, the reported TK structures show a single substrate-binding site that accommodates both dT and dTMP, demonstrating that the dT- and dTMP-sites are identical, which brings a long-lasting discussion (Chen et al., 1979b; Maga et al., 1994) to a close. Unlike the ATP/ADP-site, the nucleoside/NMP-site is totally buried in the protein interior in agreement with the low K_M value of 0.2 μM for dT (Fetzer et al., 1993; Michael, 1995). A stereoview is shown in Figure 4; the interaction scheme is given in Figure 5.

The carboxamide of Gln125 in the pocket forms hydrogen bonds with the N3 and O4α atoms of thymine. Corresponding hydrogen bonds were formed in the complex between TK and the guanosine derivative ganciclovir (Brown et al., 1995) but with the carboxamide rotated by 180° to fit the N1 and O6α atoms of guanine in its inverted binding orientation. In a further interaction Tyr172 stacks onto the thymine ring and forms a hydrogen bond to Arg163 that binds the phosphate of dTMP (Fig. 4). At the other side of its ring thymine contacts Met128.

The 3′-OH group of the ribose moiety of dT and dTMP are stabilized by hydrogen bonds to Tyr101–OH of helix α3 and to Glu225–OE1. TK accepts the L-stereoisomer of the deoxyribose of dT (Spadari et al., 1992) as well as the acyclic ribose analogues of the important anti-*Herpes* prodrugs aciclovir and ganciclovir, disclosing its low stereochemical demands for the ribose moiety.

Although thymine is bound tightly, it does not fill its binding pocket completely. In complex TK:ADP:dTMP, thymine leaves a non-polar 35 Å^3 void close to its C5 position (Fig. 6A). In TK:ADP:5-iodo-dUMP, the large iodine replaces the smaller methyl group without steric hindrance and still leaves a void of 17 Å^3 (Fig. 6B).

In the prodrug brivudin, the C5 methyl group of thymine is replaced by a bromovinyl group, which is even larger than iodine. When placing a brivudin model into the pocket using energy minimization, we found a close contact to Ala168-CB. TK from HSV-2 contains the exchange Ala168 → Ser that diminishes the binding pocket at a point where the brivudin model fits snugly and dT is not affected. This explains why the HSV-2 enzyme rejects brivudin. A similar cut into the pocket space not used by dT occurred in

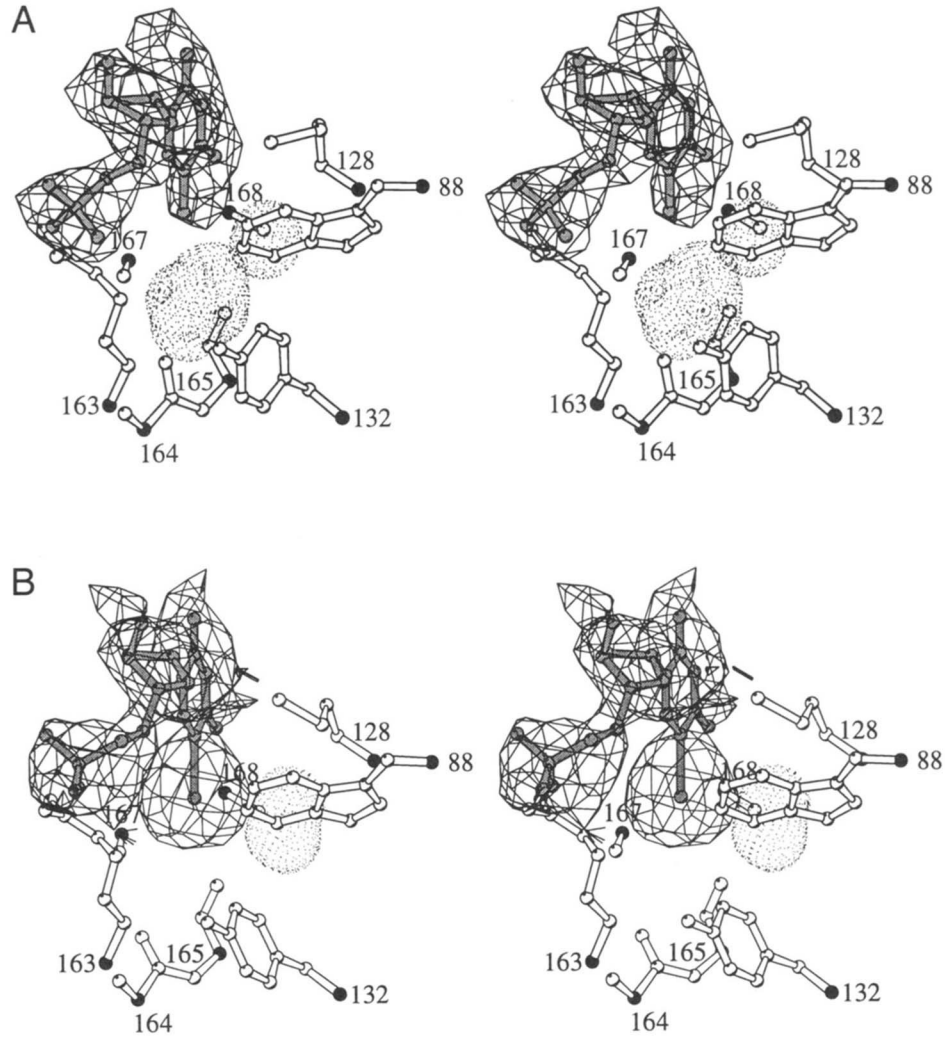

Fig. 6. Bound substrates with $(2F_o - F_c)$-densities contoured at the 1.0 σ level. The van-der-Waals surface (dotted; Connolly, 1993; 1.2 Å radius probe) of the non-polar cavity near the C5-position of the bases and the residues lining the cavity are given (C^α atoms, black; for His164 and Pro165, only the main chain). **A:** Substrate dTMP with a cavity of 35 $Å^3$. **B:** Substrate analogue 5-iodo-dUMP leaving a cavity of 17 $Å^3$.

mutation Ala168 → Thr, which was found in the TK of a brivudin-resistant strain of HSV-1 (Larder et al., 1983). This reminds us how easily a drug resistance can be developed if the drug exploits a dispensable feature of the target.

It should be noted that the O2α atom of thymine forms hydrogen bonds to two water molecules sequestered in the binding pocket (Figs. 4, 5). Sequestered water is a typical indicator for multiple substrate specificity as, for instance, observed with uridylate kinases (Müller-Dieckmann & Schulz, 1995; Scheffzek et al., 1996) that accept CMP and AMP in addition to UMP. Replacing them could improve inhibitors because water release results in an entropic gain of binding strength.

Taken together, quite a number of modifications of thymidine are tolerated without losing enzyme activity (Kit, 1985). Modified riboses and replacement by guanine (aciclovir, ganciclovir) as well as modifications at the C5 position of thymine (idoxuridine, brivudin) gave rise to prodrugs in the therapy of herpetic diseases (De Clercq, 1993). The presented TK structure may help to create others.

The two catalyzed reactions

The catalyzed phosphorylations of dT and dTMP are different reaction types because they result in an ester and an anhydride, respectively. Both reactions have similar slow rates with turnover numbers around 5 s^{-1}. The structures show that both reactions can occur successively with the phosphoryl acceptor remaining at its binding site. Structures TK:ADP:dTMP and TK:ADP:5-iodo-dUMP represent the Michaelis complex after ester formation, whereas complex TK:ADP:dT is abortive (Table 2).

A superposition of the dT and dTMP complex structures in Figure 7A shows only small differences. At 0.34 Å the RMSD of the C^α atoms is in range of the errors (Table 2). No mobile part of the molecule rigidifies significantly (Fig. 7B). The largest displacements occur around position 222, where the phosphate of dTMP pushes the backbone 1.5 Å outward (Fig. 8). The other differences of Figure 7A report structural inaccuracies caused by segmental mobility.

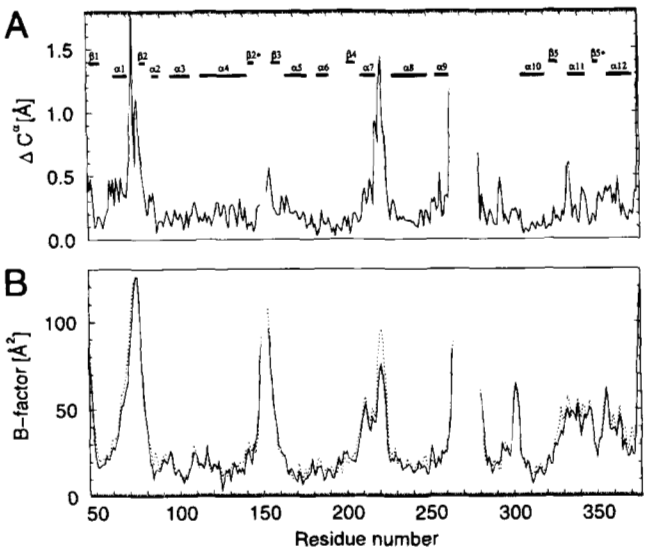

Fig. 7. Structural differences between the complexes with dTMP and dT. **A:** The residual C^{α} distances between superimposed complexes TK:ADP:dTMP and TK:ADP:dT, α-helices and β-sheets are indicated. **B:** Mobilities along the polypeptide chain for complexes TK:ADP:dT (solid line) and TK:ADP:dTMP (broken line).

Complex TK:ADP:dT suggests strongly that Glu83 functions as a base accepting the 5′-hydroxyl proton in the ester-forming reaction. In TK:ADP:dTMP, this glutamate shifts from the 5′-hydroxyl of dT to the α-phosphate of dTMP (Fig. 8). Concomitantly, Arg163 leaves its salt bridge to Asp55 and fixes the phosphate of dTMP. Furthermore, Arg220 dissociates from the α-phosphate of ADP to form a loose salt bridge to Glu225 (Fig. 4) and Arg222 leaves the β-phosphate of ADP. Less important because it is less-well defined is the displacement of Lys62-NZ away from Glu83 and towards the β-phosphate of ADP.

The presence of Asp55 just before the P-loop is a special, strongly conserved feature of the *Herpes* TK family that is absent in the homologous NMP-kinases. Obviously, Asp55 provides an internal parking place that is assumed by Arg163 when it is superfluous in the ester-forming reaction. Arg163 then leaves this place for participating in anhydride formation.

In a comparison of TK:ADP:dTMP with the NMP-kinases (see below), the oxygen atom of ADP that could accept the phosphoryl group from dTMP (ester reaction, backward) is clearly identified as O_{23} (Fig. 5). Accordingly, O_{23} of ADP and O5′ of dTMP are the anchoring atoms in phosphoryl transfer (Abele & Schulz, 1995). They are at a distance of 5.0 Å in the dTMP and of 5.1 Å in the dT complex, which is merely 0.5 Å longer than the expected distance during catalysis. Accordingly, the dT and dTMP structures provide a good description of the states before and after ester formation, respectively.

For visualizing the anhydride reaction we would need a fourth phosphate in one of our structures. Still, it is clear that O_{23} of ADP is again one of the anchors as the other two oxygens of the β-phosphoryl group are buried in the P-loop. The second anchor must be one of the three phosphate oxygens of dTMP (the 5-iodo-dUMP phosphate is essentially identical), two of which are appropriately positioned but at too short a distance from O_{23}. Because this distance is only 3 Å, the dTMP phosphate has to be displaced by 1.5–2 Å in order to assume the 4.5 Å distance between the anchor oxygens required for the anhydride reaction. In conclusion, all our structures are close to the ester reaction, and not very far from the anhydride reaction.

The thymidine kinase family

TK from HSV-1 is part of the large thymidine kinase family, which can be subdivided into herpes-viral, pox-viral, and cellular subfamilies, the sequences of which have essentially only the P-loop in common. Accordingly, one should expect only a distant evolutionary relationship among them. The members of the herpes-viral subfamily are sequence-related, however, and gave rise to several analyses (Gentry, 1985; Darby et al., 1986; Mittal & Field, 1989; Balasubramaniam et al., 1990; Folkers et al., 1991). These resulted in six homologous regions that are here denoted "motif-1" through "motif-6" (Fig. 9). Three of these six motifs are at the more general ATP-binding site while two are at the characteristic nucleoside/NMP-site.

Motif-1 is the omnipresent P-loop accommodating the β-phosphate of ATP (Fig. 3). Motif-3 (-^{161}FDRHP-; underlined means strongly conserved) contains Asp162 suspending the required Mg^{2+} ion between β- and γ-phosphate of ATP via two water molecules (Fig. 4 and Abele & Schulz, 1995). The only Asp162 exchanges retaining enzymatic activity are those to Glu and Gly (Black &

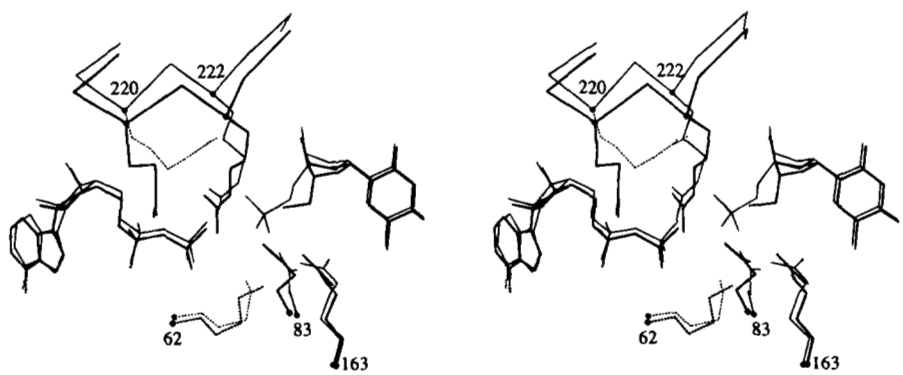

Fig. 8. Stereoview of the active site of TK:ADP:dTMP (thin lines) and TK:ADP:dT (thick lines). Residues that differ significantly (Lys62, Glu83, Arg163, Arg220, Arg222) and the C^{α} trace of LID are given. Residues containing density breaks at the 1.0 σ level are depicted with dotted lines.

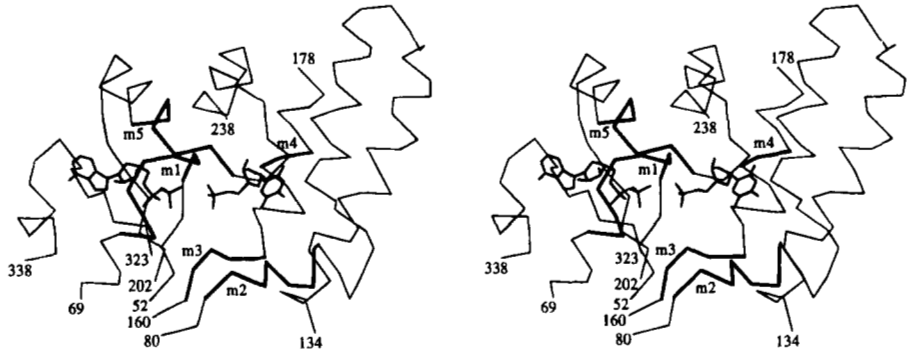

Fig. 9. Stereoview of the C^{α} trace around the active center of a TK subunit, indicating the conserved motifs of the *Herpes* viral subfamily that were extracted from the sequences (bold lines). Some residues and the motifs (m1-m5) are labeled, the substrates ADP and dTMP are included.

Loeb, 1993; Fetzer et al., 1993). Surprisingly, Pro165 forms a *trans*-peptide although the equivalent position in the NMP-kinases contains a strictly conserved *cis*-proline (Fig. 2). Motif-5 (-^{216}RLakRqR-; lower case means variable) contains Arg216 forming a sandwich with the adenine moiety of ATP and Arg220, as well as Arg222 contacting the phosphates of ATP.

Motif-2 (-^{82}PEPMtYWR-) contains Glu83, which is the putative base in ester formation. Motif-4 (-^{171}CYP-) is part of the nucleoside/NMP-binding site, its Tyr172 contacts thymine (Fig. 4). In random exchanges of Tyr172, the activity was only kept for Phe (Munir et al., 1992). The strictly conserved Pro173 interrupts the hydrogen-bonding pattern within helix α5; it is important for nucleoside binding (Munir et al., 1992). Motif-6 (-^{284}IgdTLF-) is far away from the catalytic center.

Homology to the NMP-kinases

TK contains a parallel five-stranded β-sheet with the same topology and the same P-loop as the NMP-kinases. For the NMP-kinases this part had been dubbed "CORE domain" and used for demonstrating the motions of the remaining domains "LID" and "NMP_{bind}" during catalysis (Vonrhein et al., 1995). A superposition of the C^{α} backbones of TK and AK_{yst} (Abele & Schulz, 1995) with a 3-Å cutoff resulted in 74 matched C^{α} atoms (Figs. 2, 10), which have only 24% identical residues.

Both structures contain three helices between strands β2 and β3 (Fig. 2) that form the nucleoside/NMP-binding site in TK and the NMP_{bind} domain in the NMP-kinases. The helix positions, however, differ appreciably. Between strands β3 and β4, TK has two and the NMP-kinases only one helix. After strand β4, TK and the NMP-kinases have helix α7, the LID domain, and helix α8 in common (Fig. 10). The LID of TK contains only eight residues reminiscent of the small variants of the NMP-kinases. It includes Arg220 and Arg222, which show the largest difference between dT- and dTMP-binding (Fig. 8).

The most significant deviations occur in the chain segment between helix α8 and strand β5, which in TK comprises two α-helices, two 3_{10}-helices and 15 mobile residues, adding up to 72 additional residues (Fig. 1). Helix α11 after strand β5 of TK closely resembles its counterpart, which forms the C-terminus of the NMP-kinases. In TK, this helix is followed by strand β5*, forming a short antiparallel sheet with β2*, and also by helix α12, ending at the dimer interface. Taken together, the largest differences are the additions in TK: the 45 mobile N-terminal residues, the partially mobile 72-residue-segment and the 29 C-terminal residues. Many of the differences appear to be connected to the TK dimer interface. The location of this interface differs grossly from the interface of the hitherto only structurally known dimeric NMP-kinase (Teplyakov et al., 1996).

It should be noted that all our TK structures contain both substrates, i.e., they correspond to the "closed form" of the NMP-kinases (Vonrhein et al., 1995). Therefore, it seems quite possible that substrate-free TK, like the NMP-kinases, assumes an "open form" with appreciable conformational differences.

A superposition of the 74 CORE residues (Fig. 10) brings ADP bound to TK very close to the bound ADP moiety at the ATP sites of the NMP-kinases. The crucial O_{23} oxygens that donate the γ-phosphoryl group are only 0.4 Å apart. The accepting oxygen O5′ at the nucleoside/NMP-site (ester reaction) deviates from the equivalent phosphate oxygen of the NMP-kinases only by 1 Å in the dT and dTMP complexes. Moreover, the bases of dTMP in TK and of AMP in the NMP-kinases are displaced by only 3 Å.

Taken together, the similarity of the central chain fold and of the substrate positions indicate without doubt that TK and the NMP-kinases have a common though distant ancestor in evolution, i.e., that TK belongs to the NMP-kinase family. Presumably this applies also for the greater thymidine kinase family.

Materials and methods

Recombinant TK from HSV-1 was expressed as fusion protein with glutathione-S-transferase (Fetzer et al., 1994) and purified by glutathione affinity chromatography, thrombin cleavage, and ATP-affinity chromatography. The thrombin cleavage removed 33 residues at the N-terminus. During the preparation, TK was loaded with dT (K_M = 0.2 μM) and eventually co-crystallized with 0.05 mM dT, 1.25 mM ATP, 2 mM DTT, and 1 mM EDTA (Wild et al., 1995).

Two data sets were collected at room temperature using a rotating anode (model RU200B, Rigaku) together with a multi-wire area detector (model X1000, Siemens) and processed with program XDS (Kabsch, 1988). One data set was collected at room temperature using synchrotron radiation with an image plate detector (beamline X31, EMBL outstation, Hamburg) and reduced with programs DENZO and SCALEPACK (Otwinowski, 1993).

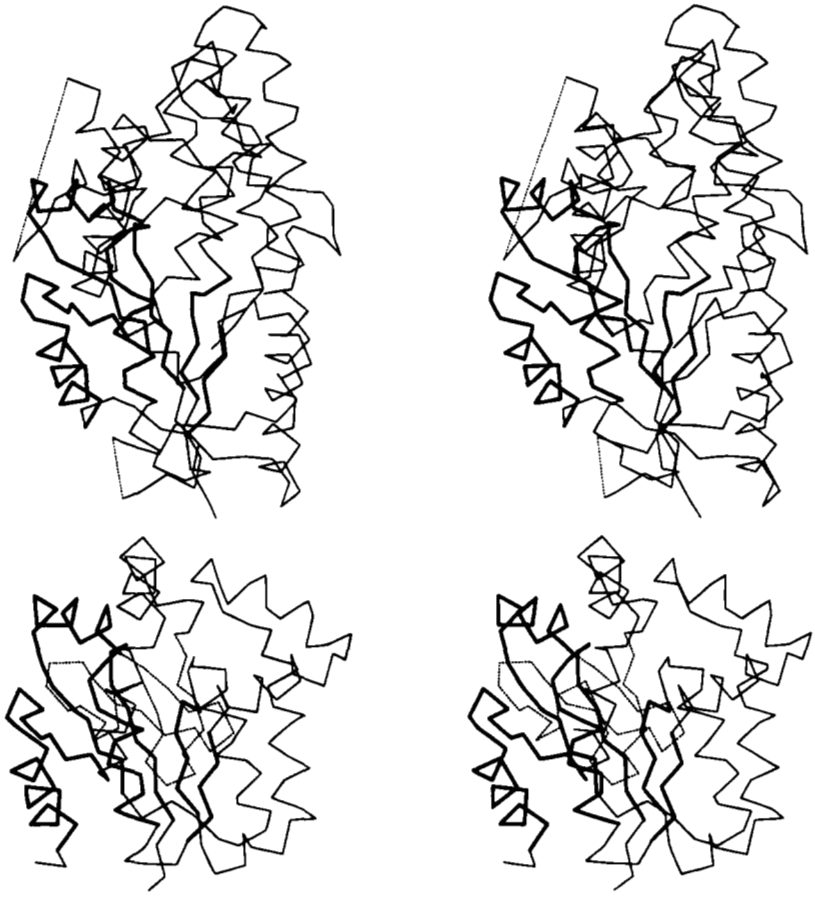

Fig. 10. Stereoview of the C^{α} traces of TK (top) and AK_{yst} (bottom) after superposition and subsequent vertical separation (for clarity). The superposition is based on 74 C^{α} atoms (residues 51–70, 78–82, 159–165, 202–220, and 323–345 of TK; Fig. 2), which are indicated by bold lines. The large LID domain of AK_{yst} is depicted using a dotted line.

The structure of TK was initially solved by multiple isomorphous replacement at 3.0 Å resolution (Wild et al., 1995). The analysis was continued with a new 2.75 Å resolution synchrotron data set of TK:ADP:dTMP. Due to the high solvent content of 67%, the parameters-to-observables ratio was good enough for individual *B*-factor refinement. At an *R*-factor of 24% we started to add water molecules at $(F_o - F_c)$-densities above 3.5 σ with at least one direct hydrogen bond to the protein. They were kept if they remained above 1.0 σ in the resulting $(2F_o - F_c)$-map. All refinements were done using X-PLOR (Brünger et al., 1987) and monitored with a free *R*-factor.

The crystal structures of TK:ADP:dT and TK:ADP:5-iodo-dUMP were established by difference-Fourier techniques (after removing all water molecules from the starting model) and subsequent refinement. Some water molecules were added using the same criteria as before (Table 2). Because of data limitation, no B-factor refinement was attempted in complex TK:ADP:5-iodo-dUMP. The coordinates are deposited in the Protein Data Bank under codes 1VTK, 2VTK, and 3VTK.

Acknowledgments

We thank S. McKnight (Tularik, South San Francisco, California) for providing us with the gene of TK from HSV-1, L. Scapozza and J.E.W. Meyer for discussions, and the team of the EMBL outstation at DESY (Hamburg) for help in collecting one of the data sets with synchrotron radiation. The project was supported by the Deutsche Forschungsgemeinschaft under SFB-60.

References

Abele U, Schulz GE. 1995. High-resolution structure of adenylate kinase from yeast ligated with inhibitor AP_5A, showing the pathway of phosphoryl transfer. *Protein Sci 4*:1262–1271.

Balasubramaniam NK, Veerisetty V, Gentry GA. 1990. Herpesviral deoxythymidine kinases contain a site analogous to the phosphoryl-binding arginine-rich region of porcine adenylate kinase; comparison of secondary structure predictions and conservations. *J Gen Virol 71*:2979–2987.

Black ME, Loeb LA. 1993. Identification of important residues within the putative nucleoside binding site of HSV-1 thymidine kinase by random sequence selection: Analysis of selected mutants in vitro. *Biochemistry 32*:11618–11626.

Brown DG, Visse R, Sandhu G, Davies A, Rizkallah PJ, Melitz C, Summers WC, Sanderson MR. 1995. Crystal structures of the thymidine kinase from *Herpes simplex* virus type-1 in complex with deoxythymidine and ganciclovir. *Nature Struct Biol 2*:876–881.

Brünger AT, Kuriyan J, Karplus M. 1987. Crystallographic R-factor refinement by molecular dynamics. *Science 235*:458–460.

Chen MS, Summers WP, Walker J, Summers WC, Prusoff WH. 1979a. Characterization of pyrimidine deoxyribonucleoside kinase (thymidine kinase) and thymidylate kinase as a multifunctional enzyme in cells transformed by *Herpes simplex* virus type 1 and in cells infected with mutant strains of *Herpes simplex* virus. *J Virol 30*:942–945.

Chen MS, Walker J, Prusoff WH. 1979b. Kinetic studies of *Herpes simplex* virus type-1 encoded thymidine and thymidylate kinase, a multifunctional protein. *J Biol Chem 254*:10747–10753.

Connolly ML. 1993. The molecular surface package. *J Mol Graphics 11*:139–141.

Culver KW, Ram Z, Wallbridge S, Ishii H, Oldfield EH, Blaese RM. 1992. In vivo gene transfer with retroviral vector-producer cells for treatment of experimental brain tumors. *Science 256*:1550–1552.

Darby G, Larder BA, Inglis MM. 1986. Evidence that the "active center" of *Herpes simplex* virus thymidine kinase involves an interaction between three distinct regions of the polypeptide. *J Gen Virol 67*:753–758.

De Clercq E. 1993. Antivirals for the treatment of Herpesvirus infections. *J Antimicrobial Chemotherapy Suppl A 32*:121–132.

Dreusicke D, Schulz GE. 1986. The glycine loop of adenylate kinase forms a giant anion hole. *FEBS Lett 208*:301–304.

Fetzer J, Folkers G, Müller I, Keil GM. 1993. Site-directed mutagenesis in the active site of the *Herpes simplex* virus type 1 thymidine kinase. *Virus Genes 7*:205–209.

Fetzer J, Michael M, Bohner T, Hofbauer R, Folkers G. 1994. A fast method for obtaining highly pure recombinant *Herpes simplex* virus type 1 thymidine kinase. *Prot Exp Purif 5*:432–441.

Folkers G, Trumpp-Kallmeyer S, Gutbrod O, Krickl S, Fetzer J, Keil GM. 1991. Computer-aided active site-directed modeling of the *Herpes simplex* virus type 1 and human thymidine kinase. *J Comp Aid Mol Design 5*:385–404.

Gentry GA. 1985. Locating a nucleotide-binding site in the thymidine kinase of vaccinia virus and of *Herpes simplex* virus by scoring triply-aligned protein sequences. *Proc Natl Acad Sci USA 85*:6815–6819.

Halpern ME, Smiley JR. 1984. Effects of deletions on expression of the *Herpes simplex* virus thymidine kinase gene from the intact viral genome: The amino terminus of the enzyme is dispensable for catalytic activity. *J Virol 50*:733–738.

Harrison PT, Thompson R, Davison AJ. 1991. Evolution of herpesvirus thymidine kinases from cellular deoxycytidine kinase. *J Gen Virol 72*:2583–2586.

Ilsley DD, Lee SH, Miller WH, Kuchta RD. 1995. Acyclic guanosine analogs inhibit DNA polymerases α, δ, and ϵ with very different potencies and have unique mechanisms of action. *Biochemistry 34*:2504–2510.

Jones S, Thornton JM. 1995. Protein–protein interactions: A review of protein dimer structures. *Prog Biophys Molec Biol 63*:31–65.

Kabsch W. 1988. Evaluation of single-crystal X-ray diffraction data from a position-sensitive detector. *J Appl Cryst 21*:916–924.

Kabsch W, Sander C. 1983. Dictionary of protein secondary structures: Pattern recognition of hydrogen-bonded and geometrical features. *Biopolymers 22*:2577–2637.

Kit S. 1985. Thymidine kinase. *Microbiol Sciences 2*:369–375.

Larder BA, Cheng Y-C, Darby G. 1983. Characterization of abnormal thymidine kinases induced by drug-resistant strains of *Herpes simplex* virus type 1. *J Gen Virol 64*:523–532.

Laskowski RA, MacArthur MW, Moss DS, Thornton JM. 1993. PROCHECK: A program to check the stereochemical quality of protein structures. *J Appl Cryst 26*:283–291.

Maga G, Focher F, Wright GE, Capobianco M, Garbesi A, Bendiscioli A, Spadari S. 1994. Kinetic studies with N2-phenylguanines and with L-thymidine indicate that *Herpes simplex* virus type 1 thymidine kinase and thymidylate kinase share a common active site. *Biochem J 302*:279–282.

McKnight SL. 1980. The nucleotide sequence and transcript map of the *Herpes simplex* virus thymidine kinase gene. *Nucleic Acids Res 8*:5949–5964.

Michael M. 1995. Biochemical characterization of wild type and mutant *Herpes simplex* virus type 1 thymidine kinase [dissertation]. Zürich: Eidgenössische Technischen Hochschule.

Mittal SK, Field HJ. 1989. Analysis of the bovine Herpesvirus type 1 thymidine kinase (TK) gene from wild-type virus and TK-deficient mutants. *J Gen Virol 70*:901–918.

Miyoshi K, Egi Y, Shioda T, Kawasaki T. 1990. Evidence for in vivo synthesis of thiamine triphosphate by cytosolic adenylate kinase in chicken skeletal muscle. *J Biochem 108*:267–270.

Müller CW, Schulz GE. 1992. Structure of the complex between adenylate kinase from *Escherichia coli* and the inhibitor AP_5A refined at 1.9 Å resolution: A model for a catalytic transition state. *J Mol Biol 224*:159–177.

Müller-Dieckmann H-J, Schulz GE. 1995. Substrate specificity and assembly of the catalytic center derived from two structures of ligated uridylate kinase. *J Mol Biol 246*:522–530.

Munch-Petersen B, Tyrsted G, Cloos L. 1993. Reversible ATP-dependent transition between two forms of human cytosolic thymidine kinase with different enzymatic properties. *J Biol Chem 268*:15621–15625.

Munir KM, French DC, Dube DK, Loeb LA. 1992. Permissible amino acid substitutions within the putative nucleoside-binding site of *Herpes simplex* virus type 1 encoded thymidine kinase established by random sequence mutagenesis. *J Biol Chem 267*:6584–6589.

Otwinowski Z. 1993. Oscillation data reduction program. In: Sawyer L, Isaacs N, Bailey S, eds. *Data collection and processing. Proceedings of the CCP4 study weekend.* Warrington, United Kingdom: SERC Daresbury Laboratory. pp 56–62.

Scheffzek K, Kliche W, Wiesmüller L, Reinstein J. 1996. Crystal structure of the complex of UMP/CMP kinase from *Dictyostelium discoideum* and the bisubstrate inhibitor P1-(5′-adenosyl)-P5-(5′uridyl)pentaphosphate (Up_5A) and Mg^{2+} at 2.2 Å: implications for water-mediated specificity. *Biochemistry 35*:9716–9727.

Schulz GE. 1992. Binding of nucleotides to proteins. *Curr Opin Struct Biol 2*:61–67.

Spadari S, Maga G, Focher F, Ciarrocchi G, Manservigi R, Arcamone F, Capobianco M, Caruro A, Colonna F, Iotti S, Garbesi A. 1992. L-thymidine is phosphorylated by *Herpes simplex* virus type 1 thymidine kinase and inhibits viral growth. *J Med Chem 35*:4214–4220.

Spadari S, Ciarrocchi G, Focher F, Verri A, Maga G, Arcamone F, Iafrate E, Manzini S, Garbesi A, Tondelli L. 1995. 5-Iodo-2′-deoxy-L-uridine and (E)-5-(2-bromovinyl)-2′-deoxy-L-uridine: elective phosphorylation by *Herpes simplex* virus type 1 thymidine kinase, antiherpetic activity, and cytotoxicity studies. *Mol Pharmacol 47*:1231–1238.

Teplyakov A, Sebastiao P, Obmolova G, Perrakis A, Brush G, Bessman MJ, Wilson KS. 1996. Crystal structure of bacteriophage T4 deoxynucleotide kinase with its substrates dGMP and ATP. *EMBO J 15*:3487–3497.

Vonrhein C, Schlauderer GJ, Schulz GE. 1995. Movie of the structural changes during a catalytic cycle of nucleoside monophosphate kinases. *Structure 3*:483–490.

Whitley RJ, Gnann JWG Jr. 1993. In: Roizmann B, Whitley RJ, Lopez C, eds. *The human Herpesviruses*. Raven, New York. pp 69–105.

WHO Meeting. 1985. Prevention and control of *Herpes* virus diseases. Part 1. Clinical and laboratory diagnosis and chemotherapy. *Bulletin of the WHO 63*:182–185.

Wild K, Bohner T, Aubry A, Folkers G, Schulz GE. 1995. The three-dimensional structure of thymidine kinase from *Herpes simplex* virus type 1. *FEBS Lett 368*:289–292.